Experimental Comparison of Optical Loss between the Silicon-on-Insulator Waveguide Corner Mirrors and Curves

DeGui Sun, Qi Zheng, Peng Liu, Trevor J. Hall

Abstract*—Based on our previous work in modeling and numerical simulations that shows the transfer efficiency of a silicon-on-insulator (SOI) waveguide corner mirror (WCM) structure can achieve 95%, this paper experimentally demonstrates the optical loss advantage of SOI WCMs over waveguide curves. Both the numerical simulations and FDTD simulations further confirm the sustainable results of more than 94% and then the manufactured devices give a 0.30dB average optical loss in experiments. In contrary, the testing results of waveguide curves show that the optical propagation loss rates of 30 and 10dB/cm require the bending radii to be 0.5 and 2.0mm, respectively.

Index Terms*— Silicon-on-insulator waveguide, waveguide corner mirror, waveguide curve, optical loss.

I. INTRODUCTION

Based on the mature microelectronic infrastructure, micro/nano-scale silicon photonic manufacturing technologies are also gradually becoming mature in the past years and attracting the increasing interests in industrial applications so that micro/nano-scale integrated silicon based optoelectronics and photonics have been forming a new essential branch of next-generation optical communications and computer systems [1], [2]. As a consequence, silicon-on-insulator (SOI) waveguides and some special structures have been adopted as a promising platform for an implementation of large-scale photonic integrated circuits (PIC) chips [2], [3]. The illustrative SOI-PIC components that have had significant progresses in device performance and applications include Fabry-Perot (F-P) micro-cavity and micro-ring based wavelength division multiplexing (WDM) components, modulators, switches and lasers [4]-[8]. For the high-performance SOI based PIC components, the ultra-small bending radii and even the corner mirror structure are preferred. Thus, in this case, the rib waveguides based sharp-bending and waveguide corner mirror (WCM) structures have more attractive interests because of their possible high optical transfer efficiencies for implementing highly integrated photonic circuits [9]-[15].

Manuscript received December,2013
This work is co-sponsored by the Idea-to-Innovation Program of NSERC Canada under Grant 395125-099 and the D&T Photonics, Inc, an Ottawa-based startup, the Natural Science Foundation China (NSFC) under Grant 60977052 and the Research Program of Ontario Centre for Excellences (OCE) of Canada. The fabrication work was supported by CMC Microsystems Canada and performed in Canadian Photonics Fabrication Centre (CPFC). A Canada start-up company - D&T Photonics (DTP), which is spun-off from University of Ottawa, also made the angel investment to this project.

All authors are with the Centre for Research in Photonics, University of Ottawa, Ottawa, Canada, and **DeGui Sun** is also with the School of Optoelectronic Engineering, Changchun University of Science and Technology, Changchun, China.

As early as in 1985, as a starting work of the WCM structure, Ogusu reported a trend with a basic discussion that the transmission efficiency of a waveguide corner structure is determined by waveguide structure and dimensions [9], and in 1991 Chung and Degli gave a relatively systematic analysis to the transfer efficiency of the WCM structure from the confinement of guided-mode in waveguides with both theoretical studies and experimental results [10]. Then, from 2002 to 2006 many research works involved the progresses of the WCM structures having micrometer and sub-micrometer dimensions that lead to an improvement of transfer efficiency [11]-[14]. In 2009, we gave a fully systematic theoretical model for studying the total internal reflection (TIR) characteristics of WCM structure by considering a combined effect of several dominant aspects [15]. In this article, we first strengthen the transfer efficiency of SOI-WCM structure with numerical and full-definite time-domain (FDTD) simulations and then we give the fabricated devices of 1x1 WCM structure having several rib waveguide dimensions and the corresponding waveguide curves in Section II. In Section III, we test optical loss performances of both the fabricated WCM structures and waveguide curves, and then give the necessary analyses for the optical loss characteristics of the WCM structure. In Section IV, we give our conclusions.

II. DEVICE CONCEPTS AND SIMULATION VERIFICATIONS FOR WCM STRUCTURE

A. Device Concepts and Theoretical Background Recall

For SOI-rib micro-scale WCM structure having a single-mode input waveguide and a single-mode output waveguide, the perspective view and top view of device are shown in Figure 1(a) and 1(b), respectively, and Figure 1(c) is the cross-sectional view of the SOI-rib waveguide used in this device structure. As shown in Fig. 1(a), a WCM structure transfers an optical beam from an input waveguide channel to an output waveguide channel at an about 90o corner angle, where θ and φ are half a corner-angle of the WCM structure and the tilt-angle of reflecting interface, respectively.

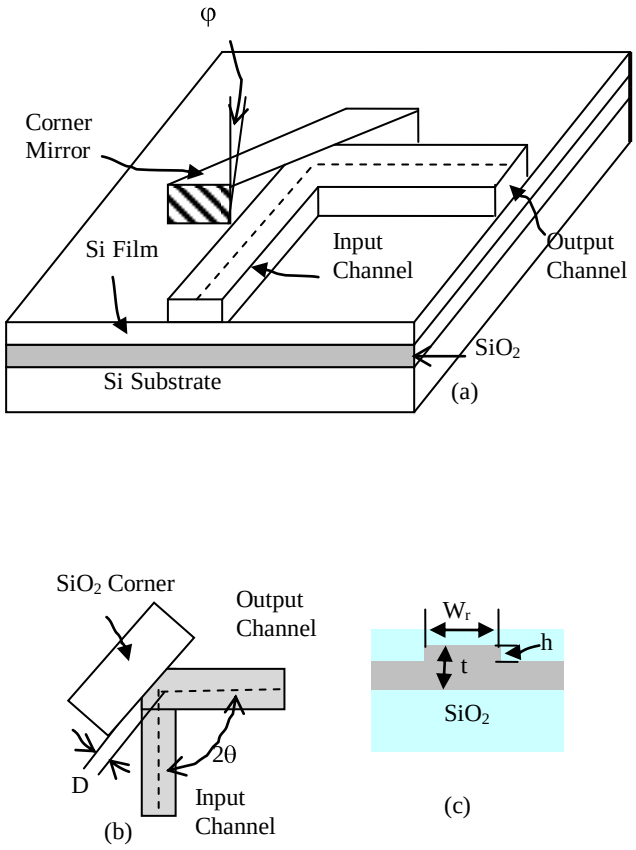

Figure 1: Schematic waveguide corner mirror (WCM) structure with physical definitions on silicon-on-insulator (SOI) waveguide platform: (a) the perspective view of WCM structure; (b) the 2D view of 1x1 WCM structure; and (c) the cross-sectional view of SOI rib waveguide, where θ is half a corner angle, i.e., incident (or reflection) angle, φ is the tilt-angle of reflecting interface of the WCM structure, and in the SOI rib waveguide, t is the silicon film thickness, h is the rib height and Wr is the channel width

As shown in Figs. 2(a) and 2(b), D is the perpendicular distance between the reflecting interface and the intersecting point of input and output waveguide channels, which is used to compensate for the Goos-Hanchen shift in the total internal reflection (TIR) process of an optical beam [15]. As shown in Figs. 1(b) and 1(c), the refractive index of waveguide core material Si is n_1 and the refractive index of cladding material SiO_2 is n_2, and the rib width of waveguides is W_r.

As we know, the reflective process of an optical beam is schematically presented in Fig. 1(b), and finally we have the reflection efficiency as [15]

$$\tau = \left| \frac{\int E_r(x_r, y_r) E_o^*(x_r, y_r) dx_r dy_r}{\int E_o^2(x_r, y_r) dx_r dy_r} \right|^2 \cdot F_\sigma \qquad (1)$$

where $F_\sigma = \exp[-(2k_o n_m \sigma \cos(\theta/2)]$ is the surface roughness induced light decay coefficient if σ denotes the roughness of the reflecting interface, $E_r(x_r, y_r)$ and $E_0(x_r, y_r)$ are the transverse electric fields of the reflected beam at reflecting interface and the fundamental mode in the output waveguide, respectively.

Our previous research shows that the effective width of the channel waveguide has an important influence on the optical transfer efficiency of the optical modal field at its reflecting interface of WCM structure and a rib waveguide structure can be equivalently changed to a channel waveguide where the effective width of the equivalent channel waveguide depends on the structure of rib waveguide [15]. The effective width of the modal field is defined by

$$W_{eff} = W_r + 2/\alpha_w, \text{ and} \qquad (2a)$$

$$\alpha_w = k_0 (n_1^2 \sin^2 \frac{\pi}{2} - n_2^2)^{1/2} \qquad (2b)$$

Further, if we only consider TE-mode, the Goos-Hanchen shift of reflected beam in this WCM structure is expressed as

$$D = \frac{1}{k_0 [n_1^2 \sin^2 (\frac{\theta}{2} + \varphi) - n_2^2]^{1/2}} \qquad (3)$$

B. Background Recall for Numerical Simulations and FDTD Verification

For the optical transfer efficiency of SOI-rib waveguide based WCM structures, our previous work has shown [15]

a. The tilt angle φ of reflecting surface for the TIR process in WCM has an impact upon the transfer efficiency of WCM structure, but it is ignorable when it is smaller than 1°.
b. The roughness σ of reflecting surface has an impact on the transfer efficiency of WCM structure, but it is ignorable when it is smaller than 100Å.
c. The Goos-Hanchen shift at the TIR surface has a critical influence on the optical transfer efficiency of this structure, namely, the transfer efficiency of WCM can reach its highest value only when the effective reflecting point of optical beam is designed at the Goos-Hanchen shift surface of about -0.15μm.
d. For an optimal SOI-based WCM structure having a tilt-angle φ of <1o, the numerical simulations show a highest optical transfer efficiency of >95% and FDTD simulations show a highest optical transfer efficiency of 94%.
e. A unique characteristic of the WCM structure is that the polarization dependence of optical transfer efficiency can be controllable with an appropriate selection of the Goos-Hanchen shift.

Figure 2 shows the FDTD simulation results of three-dimensional propagation process of E field strength of optical beam through a WCM structure with the rib waveguide having a 2.0μm rib width and 0.5μm rib height on the 1.5μm thick silicon film of SOI substrate, where (a) shows the three-dimensional style monitoring for optical beam propagation and (b) shows the single-mode profile observed at the output end port of the WCM structure, which further verifies the theoretical model and numerical values of optical transfer efficiency of the WCM structure for this work.

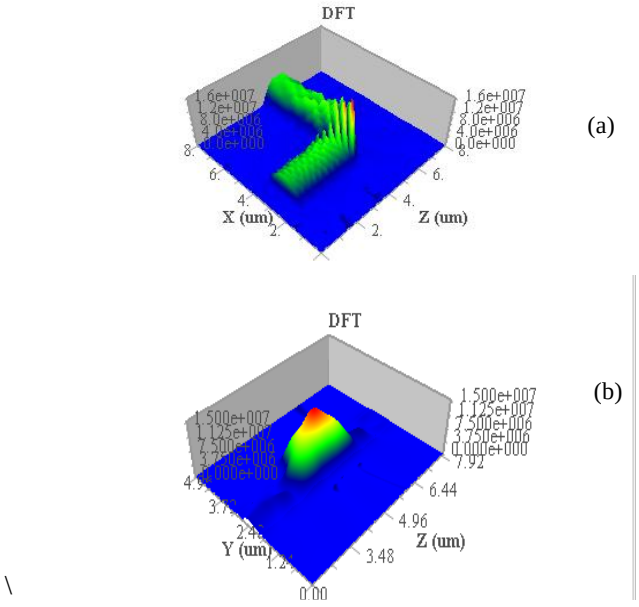

Figure 2: FDTD simulation for the SOI-based rib waveguide WCM structure where the rib height and width are designed as 0.5μm and 2.0μm, respectively: (a) the perspective optical beam propagation in an SOI-based WCM structure and (b) the 3-D profile of single-mode observed at the output end of WCM structure

At 1550nm wavelength and TE-polarization, in this work by setting the thickness of silicon film t as 1.5μm and the height of rib as 0.5μm, with equations (1) through (3) we repeat the numerical simulations for the optical intensity transfer efficiencies of WCM structure with respect to the rib width of 1.5-4.0μm and then verify that the optical transfer efficiencies of WCM structure is around 94% (0.27dB optical loss) with FDTD simulations.

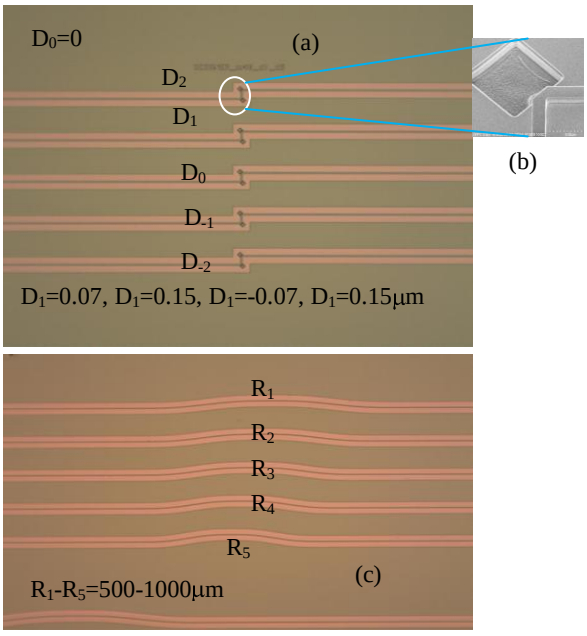

Figure 3: Layouts and distributions of two designed and fabricated structures: (a) the micro-photo of 1x1 double-corner WCM structure with 5 shifts and (b) the SEM photo of a corner structure; (c) the micro-photo of curved waveguides with 5 radii

We design and manufacture device structures – the 1x1 WCM structures and the curved waveguides, and each structure covers 6 rib widths of waveguides: 1.5-, 2.0-, 2.5-, 3.0-, 3.5- and 4.0-μm as shown in Fig. 3, where (a) and (b) illustratively show the micro-photos of 1x1 WCM structure and the curved waveguides, respectively, for the rib width of 2.0-μm, and the enlarged SEM photo of the corner mirror area is also attached to Fig. 3(a). In total, the five patterns of 1x1 WCM structure shown in Fig. 3(a) cover the 5 different values of Goos-Hanchen shift: $D = 0.0\mu m$, $D = \pm 0.07\mu m$ and $D = \pm 0.14\mu m$ to correspond with 5 relative locations of real reflecting surface of optical beam when the mirror material is set as SiO_2. As shown in Fig. 3(b), in total five designs of curved waveguides cover 5 different bending radii of 500-2000μm from the bottom to top.

III. EXPERIMENTS AND DISCUSSION

A. Experimental Setup

In accordance with our optimal designs for the WCM structure on the micron scale SOI substrate, we fabricated our devices in Canadian Photonics Fabrication Centre (CPFC), we design an experimental setup for testing the optical loss performance of fabricated waveguides and WCM structures with SOI-PIC technology as shown in Fig. 4, where a tunable laser at C+L bands, single-mode (SM) fibers and polarization maintaining (PM) fibers, a waveguide-fiber coupling/aligning station consisting of input stage, chip-carrying stage and output stage, a polarizer at signal input side and a polarization tester at signal output side, a focusing lens, a photo-detector (PD) and a displaying/analyzing system, where an infrared CCD camera for observing the output mode is also set (it is not drawn in this figure) before reading the values of optical output signals with the photo-detector. For the optical signal in the testing process of SOI-based rib waveguides and WCM structures, the polarization state is implemented with the two operations: (i) set the polarizer at the TE-state of optical signal, then launch the TE-polarized optical signal into a straight waveguide, finally adjust the polarization tester to obtain the highest output optical power value on a photo-detector; (ii) analyze the optical output signal on a Luna-system where the ratios of TE- and TM-polarization states can be separately displayed to judge the polarization state of optical signal.

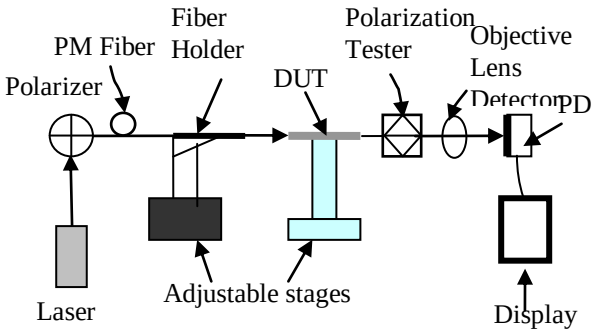

Figure 4: Schematic setup for testing the optical loss properties of SOI waveguides and WCM structures

With the detailed tests and analyses for both the stability and background noise of the experimental setup, a background stability of about 0.05dB is estimated for all the measured values of optical losses.

B. The Testing Results and Analysis

For both the 1x1 WCM structure and curved waveguide, we fabricate 6 different rib widths: 1.5-, 2.0-, 2.5-, 3.0-, 3.5-, and 4.0-μm. In this testing, our purpose is to test the optical loss values of curved waveguides and WCM structures, so it is most important to read the highest precision data of measured optical losses caused by DUT. Our measuring method includes four aspects: (i) the average optical propagation loss rate of straight rib waveguides with a cut-back method; (ii) the excess optical loss of WCM structures and (iii) the optical bending loss of curved rib waveguides. At 1550nm wavelength, the average measured optical propagation rates of linear rib waveguides (1.5-4.0μm) are around 0.8-1.2dB/cm for both TE- and TM-modes as the background values of optical loss measurements of the corresponding WCM structures and curved waveguides.

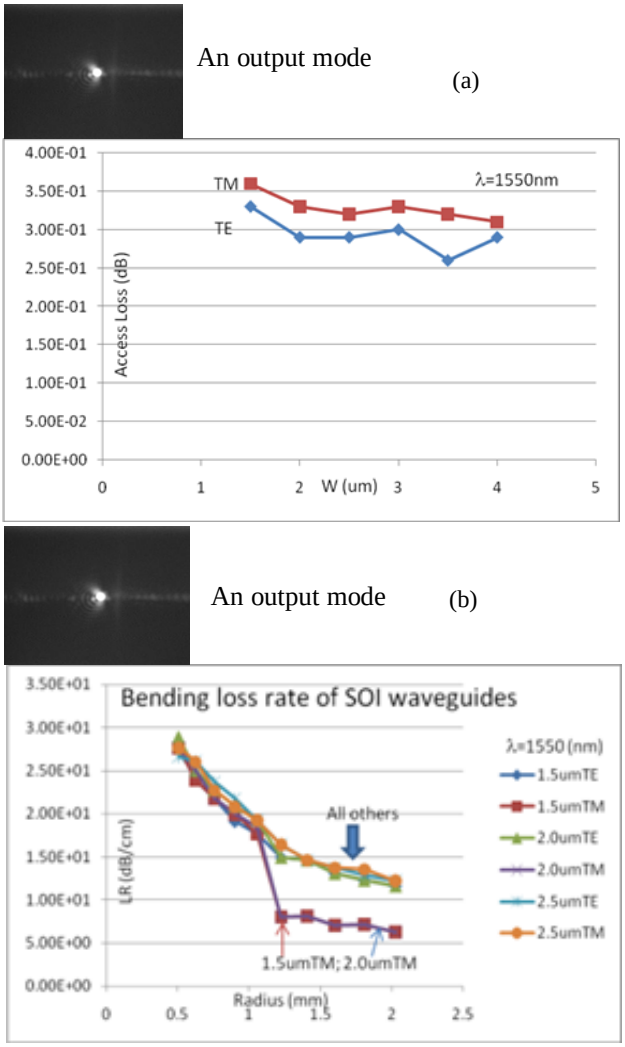

Figure 5: Testing results of two designed and fabricated structures for 6 rib widths at 1550nm wavelength for both TE- and TM-modes: (a) the 1x1 WCM structure with 5 different shifts and (b) the waveguide curves with 5 different radii, where the inset of each figure is a typical optical output mode of this structure

Then, at 1550nm wavelength we obtain the systematical testing results of optical loss of these two structures for both TE- and TM-polarizations as shown in Fig. 5, where (a) shows the optical loss of 1x1 WCM structure for all the 6 rib widths of waveguides and (b) shows the dependence of optical propagation loss rates on the bending radius for all the 6 rib-widths of waveguides curves. Note from Fig. 5(a) that the average excess optical loss of 1x1 WCM structure is 0.28 and 0.32dB for TE- and TM-polarization, respectively, namely, the average polarization dependent loss (PDL) is around 0.04dB. In fact, this PDL value of 0.04dB can only be used to estimate the possible PDL value because of the 0.05dB stability of experimental setup. Note from Fig. 5(b) that the optical propagation loss rate of a curved waveguide strongly depends on the bending radius.

When the radius is around 0.5mm, the optical propagation loss rate is around 30dB/cm for all the 6 rib widths of waveguides, and even when the radius is increased to 2.0mm, the optical propagation loss rates of these curved waveguides are around 10dB/cm. In fact, as mentioned above, with straight waveguides and cut-back method, we have obtained that the optical propagation loss rates of the straight waveguides in the rib-width range of 1.5-4.0μm are at the range of 0.8-1.2dB/cm. So, we conclude the bending structures of SOI waveguides really cause an impressively extra optical loss based on the optical propagation loss of straight waveguides, then the relatively large radii must be adopted to yield to the waveguide bending caused extra optical propagation loss in the designs of real SOI-PIC devices. Thus, such large radii of curved waveguides must lead to the much larger circuit layout than the counterpart of WCM structure in the design of a variety of PIC devices. To the contrary, the excess optical loss of each WCM structure is fixed around 0.3dB, which is significantly conducive to the complicated designs of SOI-PIC devices in several aspects such as compressing the layout size, reducing the optical on-chip loss budget and improving the performance uniformity. In addition, in Fig. 5(b) the bigger values of the bending caused excess optical propagation loss values make the polarization dependence of optical propagation loss rates ignorable in device designs.

IV. CONCLUSION

This work executes an experimental verification of our previous work in theoretical modeling and numerical simulations, so it strongly demonstrates the combinative effect of the accurate modeling and systematical simulations of WCM structure in guiding the device design and fabrication with SOI-rib waveguide technology at first. Then, it has experimentally verified the effectiveness of the WCM structure in reducing the circuit layout size and complexity compared with the waveguide curves, leading to the higher integrity and uniformity of SOI-PIC devices. As a sequence, this work has demonstrated the advanced characteristics of SOI-PIC based WCM structure and WCM-based components in both optical performance and their substantial applications in future silicon photonic networks-on-chip (NoC).

ACKNOWLEDGMENT

Authors would like to thank Dr. Jessica X. Zhang, the CMC Microsystems of Canada for her helps in the fabrication of devices by executing the program with the Canadian Photonics Fabrication Centre (CPFC). In testing work, authors also got friendly helps from the other co-workers, including Julie Nkanta, Nic Olivieri, Imad Hasan, Robert Radziwilowicz, and Ewa Lisicka.

REFERENCES

[1] B. Jalali and S. Fathpour, "Silicon photonics," J. Lightw. Technol., vol. 24, Jun. 2006, pp. 4600-4615.
[2] L. Chen, K. Preston, S. Manipatruni, and M. Lipson, "Integrated GHz silicon photonic interconnect with micrometer-scale modulators and detectors," Opt. Exp. Vol. 17, 2009, pp. 15248-15256.
[3] T. Maruyama, T. Okumura, S. Sakamoto, K. Miura, Y. Nishimoto, and S. Arai, "GaInAsP/InP membrance BH-DFB lasers directly bonded on SOI substrate,". Opt. Exp. vol. 14, 2006, pp. 8184-8188.
[4] J. Niehusmann, A. Vorckel, P. H. Bolivar, T. Wahlbrink, and W. Henschel, "Ultrahigh-quality-factor silicon-on-insulator microring resonator," Opt. Lett. vol. 29, 2006, pp. 2861-2863.
[5] J. V. Campenhout, W. M. J. Green, S. Assefa, and Y. A. Vlasov, "Low-power, 2x2 silicon electro-optic switch with 100-nm bandwidth for broadband reconfigurable optical networks," Opt. Exp. Vol. 17, 2007, pp. 24020-24029.
[6] A. Liu, R. Jones, L. Liao, D. Samara-Rubio, D. Rubin, O. Cochen, R. Nicolaescu, and M. Paniccia, "A high-speed silicon optical modulator based on a metal-oxide-semiconductor capacitor," Nature vol. 427, 2004, pp. 615-618.
[7] R. Chen, T.-T. D. Tran, K. W. Ng, W. S. Ko, L. C. Chuang, F. G. Sedgwick, and C. Chang-Hasnain, "Nanolasers grown on silicon,". Nat. Photon. vol. 5, no. 1, 2011, pp. 170-175.
[8] T. Yin, R. Cohen, M. M. Morse, G. Sarid, Y. Chetrit, D. Rubin, and M. J. Paniccia, 2007. "31-GHz Ge n-i-p waveguide-photodetectors in silicon-on-insulator substrate," Opt. Exp. vol. 15, 2007, pp. 13965-13971.
[9] K. Ogusu, "Transmission characteristics of optical waveguide corners," Opt. Commun. Vol. 55, 1985, pp. 149-153.
[10] Y. Chung and N. Dagli, "Analysis of integrated optical corner reflectors using a finite-difference beam propagation method," IEEE Photon. Technol. Lett. vol. 3, 1991, pp.150-152.
[11] R. U. Ahamd, F. Pizzuto, G. S. Camarda, R. L. Espinola, H. Rao, and R. M. Osgood, "Ultracompact corner-mirrors and T-branches in silicon-on-insulator," IEEE Photon. Technol. Lett. vol. 14, 2002, pp. 65-67.
[12] W. M. J. Green, M. J. Rooks, L. Sekaric, and Y. A. Vlasov, "Ultra-compact, low RF power, 10Gbps silicon Mach-Zehnder modulator," Opt. Exp. vol. 15, 2007, pp. 17106-17113.
[13] S. Ladenois, D. Pascal, L. Vivien, E. Cassan, S. Laval, R. Orobtchouk, M. Heitzmann, N. Bouzaida, and L. Mollard, "Low-loss submicrometer silicon-on-insulator rib waveguides and corner mirrors," Opt. Lett. vol. 28, 2003, pp. 1150-1152.
[14] Y. Qian, S. Kim, J. Song, and G. P. Nordin, "Compact and low loss silicon-on-insulator rib waveguide 90° bend," Opt. Exp. vol. 14, 2006, pp. 6020-6028.
[15] D.-G. Sun, X. Li, D. Wong, Y. Hu, F. Luo, and t. J. Hall, "Modeling and numerical analysis for silicon-on-insulator rib waveguide corners," J. Lightw. Technol. vol. 27, no. 20, 2009, pp.4610-4618.